J. Fluid Mech. (1985), *vol.* 161, *pp.* 329–346
Printed in Great Britain

Evaporation of volatile-liquid lenses floating on an immiscible-liquid surface: effects of the surface age and fluid purities in *n*-pentane/water system

By T. NOSOKO, T. OHYAMA AND Y. H. MORI
Department of Mechanical Engineering, Keio University, Yokohama 223, Japan

(Received 11 October 1984 and in revised form 20 June 1985)

This paper describes a fundamental study of evaporation of volatile-liquid lenses due to the heat supply from the substrate of an immiscible, less-volatile liquid under the atmosphere of the common vapours of the two fluid substances. Experiments were performed with single *n*-pentane lenses placed on the surface of an otherwise quiescent pool of water. The behaviour of each lens throughout its life was observed in detail using laser shadowgraphy. It was found that the time required for complete evaporation of each lens and the behaviour of the lenses change, in a peculiar but rather regular way, with the age of the water surface. This ageing effect is more significant when fluids of higher purities are used, and it is thought to be due to the quantity of contaminants at the surface increasing with its age.

1. Introduction

This study deals with the evaporation of single volatile-liquid lenses placed on the surface of an otherwise quiescent pool of immiscible, denser, less-volatile liquid. The volatile liquid, which is assumed to have surface tension well below that of the other liquid, forms fairly thin biconvex lenses (Langmuir 1933). The system temperature or the bulk temperature in the substrate liquid is maintained somewhat higher than the saturation temperature of the volatile liquid corresponding to the system pressure, while the space above the substrate liquid is filled with nearly saturated common vapours of the two liquids. Thus, the heat transfer from the substrate liquid to each lens is exclusively or, at least, primarily responsible for the evaporation of the lens.

This kind of problem has a practical importance in relation to one type of direct-contact evaporators, which has potential applicabilities in, for example, water desalination units, geothermal-heat-recovery systems and waste-heat-recovery systems. It has been studied so far by Bentwich, Landau & Sideman (1970), Kodres, Jacobs & Boehm (1979, 1980), and Kaneko & Mori (1984). Bentwich *et al.* analysed quasi-steady heat conduction through a quiescent substrate-liquid layer of semi-infinite extent to a lens. The lens shape was assumed to be oblate spheroidal, and the temperature in the lens was assumed to be uniform. They also performed experiments with isopentane lenses on water. The experimental values of the rate of shrinkage of lens radius scattered widely and were generally 3.5 times higher than predicted values based on their theoretical analysis mentioned above. Kodres *et al.* (1979, 1980) dealt with the same process but with a substrate-liquid surface in contact with a ternary air/vapour/vapour mixture. They performed a numerical analysis assuming a transient heat conduction through a stationary liquid layer of semi-infinite extent to an evaporating surface of a circular-disk-shaped lens of a volatile liquid. The lens thickness was assumed constant, and the resistance to conduction through the lens was taken into account. Their experimental evaporation times with *n*-pentane lenses on tap water, geothermal brine or glycerol were appreciably shorter than those predicted by their numerical analysis. More recently Kaneko & Mori (1984) performed experiments with *n*-pentane or R 113 (trichlorotrifluoroethane) lenses on water contacting with saturated common vapours of the two liquids. They found no change of evaporation rate when the water-layer thickness was stepped down to 1.6 mm, and thus presumed that the buoyancy-driven convection did not play an important role. They found also that *n*-pentane lenses often became unstable while R 113 lenses were always stable. The evaporation rate of *n*-pentane lenses was typically 10 times higher than that of R 113 lenses under the same temperature driving force. Kaneko & Mori suggested that such a remarkable difference in evaporation rate between *n*-pentane and R 113 lenses was ascribable to a kind of interfacial turbulence which caused the unstable behaviour of *n*-pentane lenses. However, they did not identify its mechanism.

We note that, throughout those previous studies, (i) experimental data obtained under nominally the same conditions in each study scatter widely, and (ii) experimental data showed an evaporation rate for each lens which is appreciably higher than the theoretical prediction based on a purely conductive heat-transfer assumption. The present study has been motivated by these points, which have not yet been clearly explained. In our experiments we employed the combination of *n*-pentane and water; and we paid special attention to the degree of contamination in the system, particularly that at the surface of the substrate liquid, the water. It is well known that the physico-chemical nature of fluid interfaces is highly sensitive to a trace amount of impurities in the fluids (Mysels & Florence 1970) and that 'cleanness' of the interfaces depends on their 'age' (Detwiler & Blanchard 1978). Thus, we employed a few fluid samples of different purity levels for comparison, and noted the dependence of evaporation behaviour on the age of the water surface.

2. Experiments

A schematic diagram of the experimental apparatus is shown in figure 1. The main portion of the apparatus consisted of a rectangular water bath with a cylindrical evaporation chamber submerged in it. Both of them were fabricated of plates and pipes of transparent polymethylmethacrylate. Inside, the evaporation chamber had a diameter of 190 mm and height of 150 mm. In the chamber a pipe of 140 mm inside diameter and 100 mm height was welded on the bottom plate to form a cylindrical annulus. The core section of the annulus was filled with water, which served as the substrate liquid. A magnetic stirring rod (not shown in figure 1) was immersed in the water pool to expedite the recovery of the temperature field after each lens evaporation. The water surface could readily be renewed if necessary by feeding additional water from an external reservoir into the water pool to flood it.

The *n*-pentane vapour was supplied to the evaporation chamber, at a flow rate of 5–15 cm^3/s, from a Pyrex boiler through connecting tubes made of Pyrex and Teflon. The vapour was superheated, while flowing in the connecting tubes, up to near the prescribed level of water bulk temperature T_∞ in the evaporation chamber. Because of this superheating of the *n*-pentane vapour the temperature in the water pool beneath could be held uniform to within 0.1 K right up to the surface. The vapour

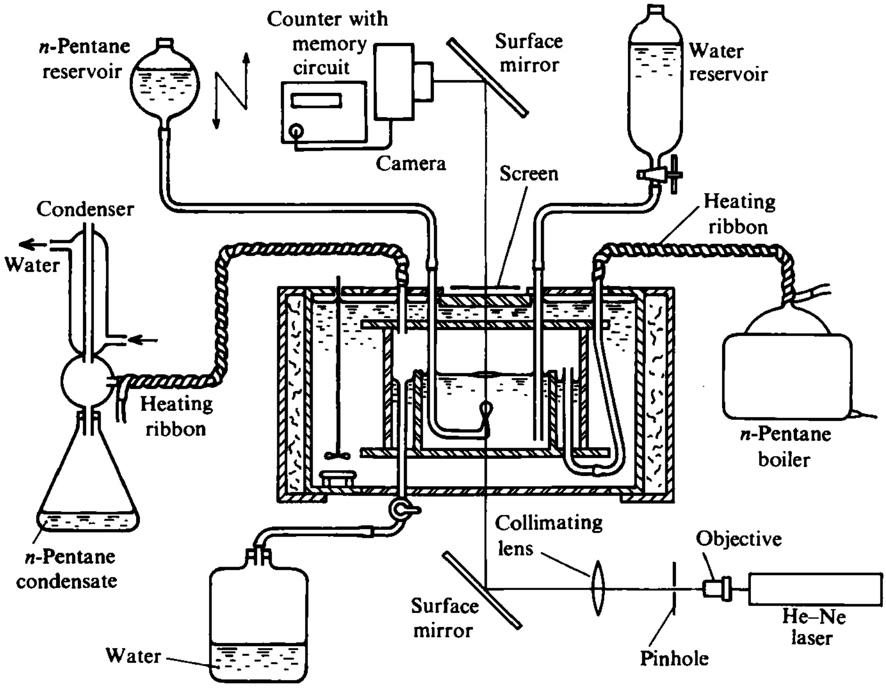

FIGURE 1. Schematic diagram of experimental apparatus.

was then passed directly into an external condenser which was open to the atmosphere. Thus, the pressure inside the chamber p_∞ was well approximated by the atmospheric pressure in the laboratory.

The liquid *n*-pentane to form lenses was supplied through a Pyrex nozzle immersed in the water pool. The *n*-pentane was presumed to be so superheated as to thermally equilibrate with the surrounding water before its release from the nozzle tip into the water in the form of single drops. Each drop rose in the water, arrived at the surface and, after some time lapse (typically several seconds) till the rupture of a water film separating the drop and the vapour phase, suddenly burst to form a lens. By employing either of two nozzles of different diameters, we produced lenses of two levels of initial volume V_0: one was 14–16 mm^3 and the other was 47–50 mm^3. Though this method of lens formation is different from that to be used in practical direct-contact evaporators, it is quite adequate to specify the inception of each evaporation process and to obtain reproducible results.

The evaporation behaviour of each lens was observed by the same technique of laser shadowgraphy as Yang & Nouri (1981) used in their study of evaporating drops on a hot solid plate. A 5 mW He–Ne laser was used as the light source. The laser beam was expanded to 42 mm diameter through a collimating lens and passed through the evaporation chamber vertically from bottom to top. It was intercepted by a horizontal ground-glass screen placed above the chamber. The image on the screen was recorded by a 35 mm motor-driven camera assembly as described in Higeta, Mori & Komotori (1979). Figure 2 illustrates the geometrical relation between a lens on the water surface and its image on the screen. The rays passing through the lens of diameter D form a bright circle of diameter D_{in} on the screen while the rays passing through the external water meniscus brighten an area, on the screen, outside of the diameter D_{out}, thus forming a dark ring bordering the two bright areas. Clearly

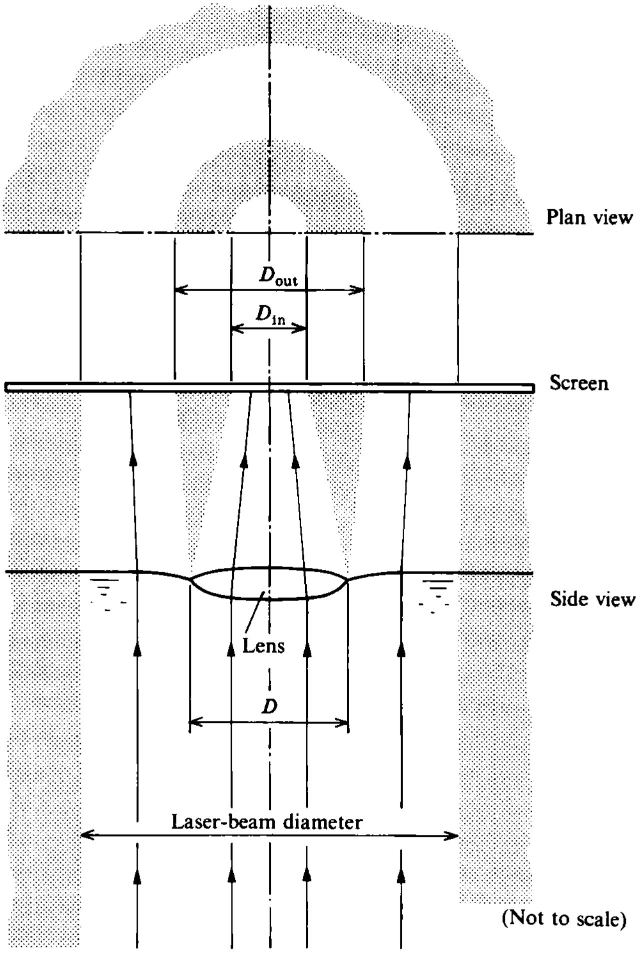

FIGURE 2. Illustrative diagram of geometric relation between a lens on the water surface and its image on the screen.

$D_{out} > D > D_{in}$. However, it was found through preliminary experiments using simultaneous recordings of evaporating lenses by the shadowgraphy and direct photography that D and D_{out} agreed to within a measuring error in the present system. Thus, in most of the later experiments we used only the shadowgraphy by which we measured D_{out} and regarded it as D, the lens diameter (or, when the lens periphery was not circular, the equivalent circular diameter of lens). It should be noted also that the morphologies of the top and bottom surfaces of each lens as well as the flow structure inside the lens would be expected to be portrayed in the inner bright area inside D_{in} on the screen.

Before each series of experiments the evaporation chamber was taken apart, cleaned and then assembled again. The cleaning process before reassembly was as follows. First we washed the components of the chamber for more than 5 min in an ultrasonic cleaning bath that had been filled with an aqueous solution of a surface-active cleaning agent. They were then rinsed in the same bath under ultrasonics for more than 5 min while the cleaning solution was continuously replaced with tap water. After that they were again rinsed with a large quantity of running tap water. Finally they were rinsed with the same purified water as used in the experiments and then dried in a vacuum chamber. After they were dried, those that were to contact with liquid *n*-pentane in the experiments were washed with the same *n*-pentane sample as the one to be used. Great care was taken to prevent the inside surfaces of the chamber as well as the surfaces of connecting tubes inserted in the chamber from being contaminated with human skin oil, particularly during the assembling operation. After the assembly *n*-pentane vapour and water from the same samples to be used in the subsequent experiments were passed through the chamber for over 15 h for the purpose of final cleaning. In our experience the final cleaning operation over a sufficiently long time was critical for obtaining reproducible results, rather than the cleaning of the components before their assembly.

Each series of experiments started with a renewing of the water surface in the evaporation chamber by means of flooding. Once the apparatus was cooled down and the air was introduced into the evaporation chamber after the final cleaning process, the apparatus was heated again till the water temperature in the chamber approached a prescribed level. Then the supply of *n*-pentane vapour was started. After several hours of supplying vapour, and, at the same time, after the fluctuation of water temperature T_∞ measured by a copper–constantan thermocouple reached within 0.3 K around the prescribed level, the following procedure was followed and repeated: (i) an *n*-pentane drop was released from the nozzle; (ii) as the drop burst at the water surface, turning into a lens, the photographing was started and, at the same time, the lifetime of the lens was measured using a stopwatch; (iii) after the evaporation was completed, 0–200 drops were released successively from the nozzle in order to promote the ageing of the water surface through the evaporation of these drops; and (iv) the water phase was mixed by the magnetic stirrer for 1 minute or less, and then left to stand for 10 min to calm it before the release of the next drop. In some series of experiments, this sequential procedure was interrupted once at a particular age of the water surface by an operation of surface renewal by flooding, and then the procedure was resumed.

Two different grades of both *n*-pentane and water were used, namely *n*-pentane of 95.0% wt certified purity as received from its manufacturer and *n*-pentane of 99.0% certified purity, distilled once in an all-glass distillation apparatus before use; tap water as received and tap water purified with commercial equipment, which comprises a reverse-osmosis device and an ion-exchange device as well as an all-glass distillation unit.† We tested three combinations of these samples as listed in table 1. It should be noted that in each experiment the same *n*-pentane sample was used to form lenses and to generate vapour in the external boiler.

The saturation temperature of *n*-pentane T_{1s} under atmospheric pressure (101.3 kPa) is 36.1 °C. However, the temperature at the evaporating surface of

---

† Note that the water-purification method that we used in the present work may not be the best for the purpose of removing surface-active materials. We later did a 'bubble persistence test' (Kitchener & Cooper 1959) by shaking a water sample obtained by the above purification method in a clean flask. Most air bubbles trapped in the water burst within 0.5 s every time they rose to the free surface, but sometimes a few bubbles persisted for several seconds. This result indicates that our 'purified water' should not always be considered free from surface-active impurities, though the static-surface-tension values of water purified by the same method agreed with the values recommended by the IAPS (1976) within a deviation of 0.26 mN/m over the range 15–60 °C (Mori, Tsui & Kiyomiya 1984). Better purification may be obtained by either of the following operations used after a first distillation: (i) a second distillation from an oxidizing aqueous solution, or (ii) passing the water through a bed of activated charcoal. We thank a referee for telling us about the bubble persistence test and the alternative purification techniques.

System	n-Pentane	Water
A	99.0 % certified purity, distilled	Purified by reverse osmosis, ion-exchange and distillation
B	95.0 % certified purity	Purified by reverse osmosis, ion-exchange and distillation
C	95.0 % certified purity	Tap water

TABLE 1. Combinations of fluid samples

n-pentane lenses must be lower than T_{1s} because of the presence of water vapour. The possible lower limit of the evaporating-surface temperature is given by the 'system saturation temperature' T_s which is defined as a temperature T such as to satisfy the following relation:

$$p_{1s}(T)+p_{2s}(T) = p_\infty,$$

where $p_{1s}(T)$ and $p_{2s}(T)$ denote saturated vapour pressures of n-pentane and water respectively at temperature T, and p_∞ denotes the system pressure, which we assume to be equal to the laboratory pressure. When $p_\infty = 101.3$ kPa, $T_s = 34.3$ °C. The nominal temperature difference ΔT, which we use later, is defined as the excess of undisturbed water temperature T_∞ over T_s.

3. Results and discussion

3.1. *Water-surface ageing: its effect and mechanisms*

It was found that the evaporation time (the time lapse after formation of each lens till the completion of evaporation of the lens) t_v, as well as the behaviour of lenses during their evaporation, strongly depended on the age of the water surface (i.e. the time lapse after the last renewal of the water surface by flooding). The dependence was most remarkable in the most purified system, i.e. system A listed in table 1. Some results for that system are presented first.

Figure 3 shows the variation of evaporation time t_v with the age of the water surface. Note that between the taking of any two adjacent data points at ages higher than 7.4 h on the graph, 4–10 drops were supplied to the water surface and, after turning into lenses, evaporated. Over the first 7.4 h of the surface age no drop was supplied to the surface except the seven drops which are represented by the first seven points on the graph. The ageing of the water surface is presumably related to the adsorption and/or sedimentation of n-pentane and contaminants on the surface. These adsorbates and sediments possibly came from the water bulk and the vaporous phase as well as the lenses fed to the surface. Thus, we can expect that the instantaneous state of ageing depends on both the time lapse and the number of lenses that have evaporated away on the surface up to that time. (As a matter of fact, we confirmed through a series of experiments that the ageing could be expedited by supplying lenses at higher frequencies.) It should be noted accordingly that a t_v profile such as shown in figure 3 is scaled up or down in the abscissa, keeping approximately its relative shape, depending on the frequency of supplying lenses.

The lifetime of the water surface may be divided into four stages (from stage I to stage IV), as indicated in figure 3, depending on the change in t_v and on the behaviour of the lenses during their lives. This is explained below with the help of figures 4–7. Figure 4 shows the changes with time of equivalent circular diameters of lenses during

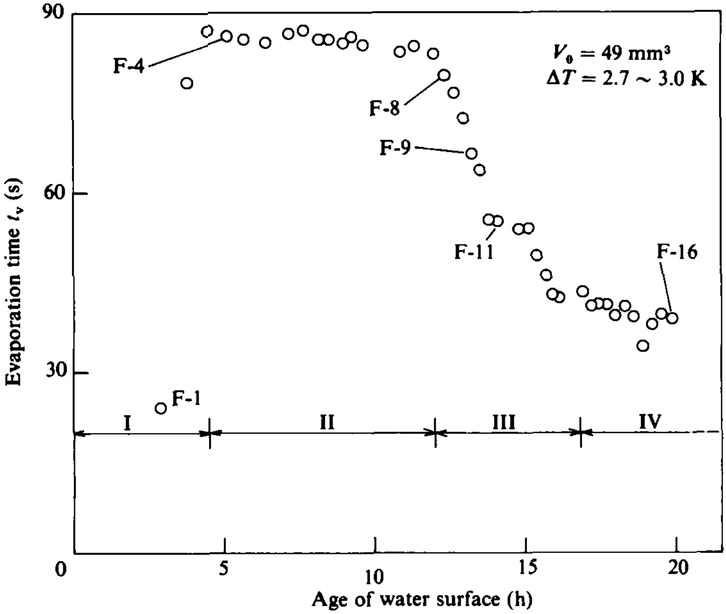

FIGURE 3. Typical variation of evaporation time with the age of water surface for system A (see table 1). Roman numerals (I–IV) in the graph specify characteristic stages into which the life of the water surface may be divided (see text). Some runs (F-1–F-16) are specified for which evaporation histories are given in figure 4.

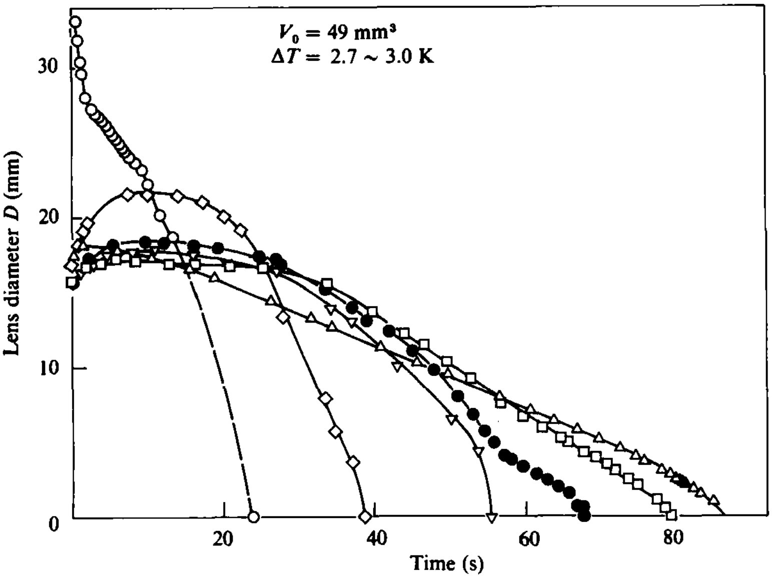

FIGURE 4. Changes of equivalent spherical diameters of lenses throughout their lifetimes at different ages of the water surface: ○, run F-1; △, F-4; □, F-8; ●, F-9; ▽, F-11; ◇, F-16.

their lives in some particular runs, which are indicated in figure 3. Figures 5–7 are shadowgraphs of evaporating lenses.

Stage I is characterized by an immediate spreading of *n*-pentane liquid when a drop bursts at the water surface. Then the *n*-pentane liquid either vanishes in quite a short time or, in a later part of stage I, contracts rapidly into a lens. The latter case is exemplified by run F-1. As the age advances, the extent of the initial spreading decreases, and t_v increases. The border between stage I and stage II is defined as a critical age beyond which t_v levels off and at the same time the initial spreading fails to happen. Throughout stage II t_v is almost constant; to be more exact, it continues to decrease only gradually. The contour of each lens remains circular throughout its life (see figure 5), and its diameter decreases linearly with time over the major part of the life (see figure 4). The end of stage II is specified by the start of a sudden drop in t_v towards a much lower level than that maintained in stage II. The range of the age in which t_v undergoes the drop toward a new level is identified as stage III. In each evaporation process during stage III, D first increases and then decreases, generally at an increasing rate, thus yielding on a (D, time)-plane a locus which is convex upward; this is demonstrated by the results of runs F-8–F-11 in figure 4. The increase of D over the initial lens diameter indicates an appreciable thinning of each lens, at least during a part of its life. The lens contour is not always circular but is distorted in a later part of the lens life (figure 6). The range of the age after t_v has approximately approached the new, lower level is identified as stage IV. In this stage the lens behaviour observed in stage III becomes more pronounced. The formation of a lens is succeeded by an appreciable increase in D over the initial diameter, which is unexpectedly almost constant irrespective of the age of the water surface. The lens has an irregular unstable contour in a later part of its life after D reaches a maximum (figure 7). Some vertical ridges at the lens surface can also be seen in a peripheral region of the lens. Shorter evaporation times in stages III and IV compared with those in stage II are presumably related to the increase in D of each lens beyond its initial diameter, resulting in a larger surface area and a smaller thickness, and to the irregular distortion of lens configuration, which must be accompanied by some convection effect.

We have explained so far the changes in evaporation behaviour with the age of the water surface once it is formed. The ageing is interrupted and is set back to a new starting point if we renew the water surface by making only the surface layer of the water pool overflow. The restart is then succeeded by an ageing history similar to its predecessor.

The mechanisms of the ageing over the four stages are of great interest. There is little doubt that the ageing through stages II, III and IV is ascribable to an accumulation of some contaminants at the water surface. Possible ways for the contaminants to accumulate are briefly discussed in the next subsection. The controlling mechanism behind the ageing during stage I, in which the most drastic change both in evaporation behaviour and evaporation time is experienced is, however, disputable. Here we present two alternative hypotheses. Hypothesis (i) assumes the adsorption of *n*-pentane molecules at the water surface to be still incomplete in stage I, thus permitting *n*-pentane liquid to spread on the water surface. (It should be noted that even such a minute undersaturation of the adsorption as to give the water surface tension a value higher by only 0.1 mN/m than the value to be obtained under exactly saturated condition may be sufficient to cause a spreading of the *n*-pentane liquid instead of lens formation.) As the adsorption is promoted by a few *n*-pentane drops supplied to the water surface, the driving force

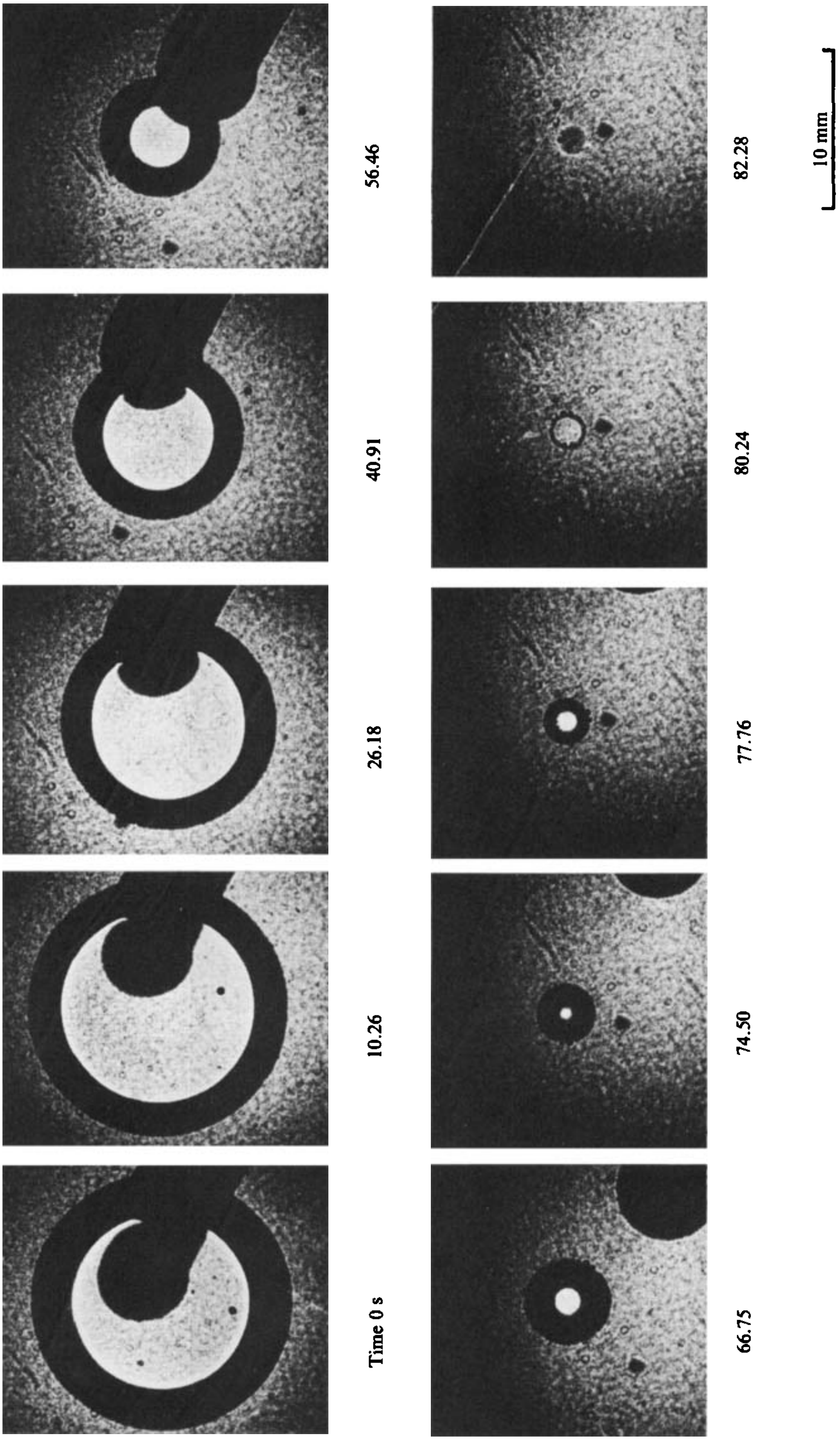

FIGURE 5. Shadowgraphs of an evaporating lens. Run F-4 (see figure 3). Consult figure 2 and the relevant description in §2 in the text for interpreting the lens images. The black bar with a round tip is the shadow of the nozzle submerged in the water pool (see figure 1). The change of location of the lens relative to the nozzle indicates that the lens was not stationary but migrating during the evaporation.

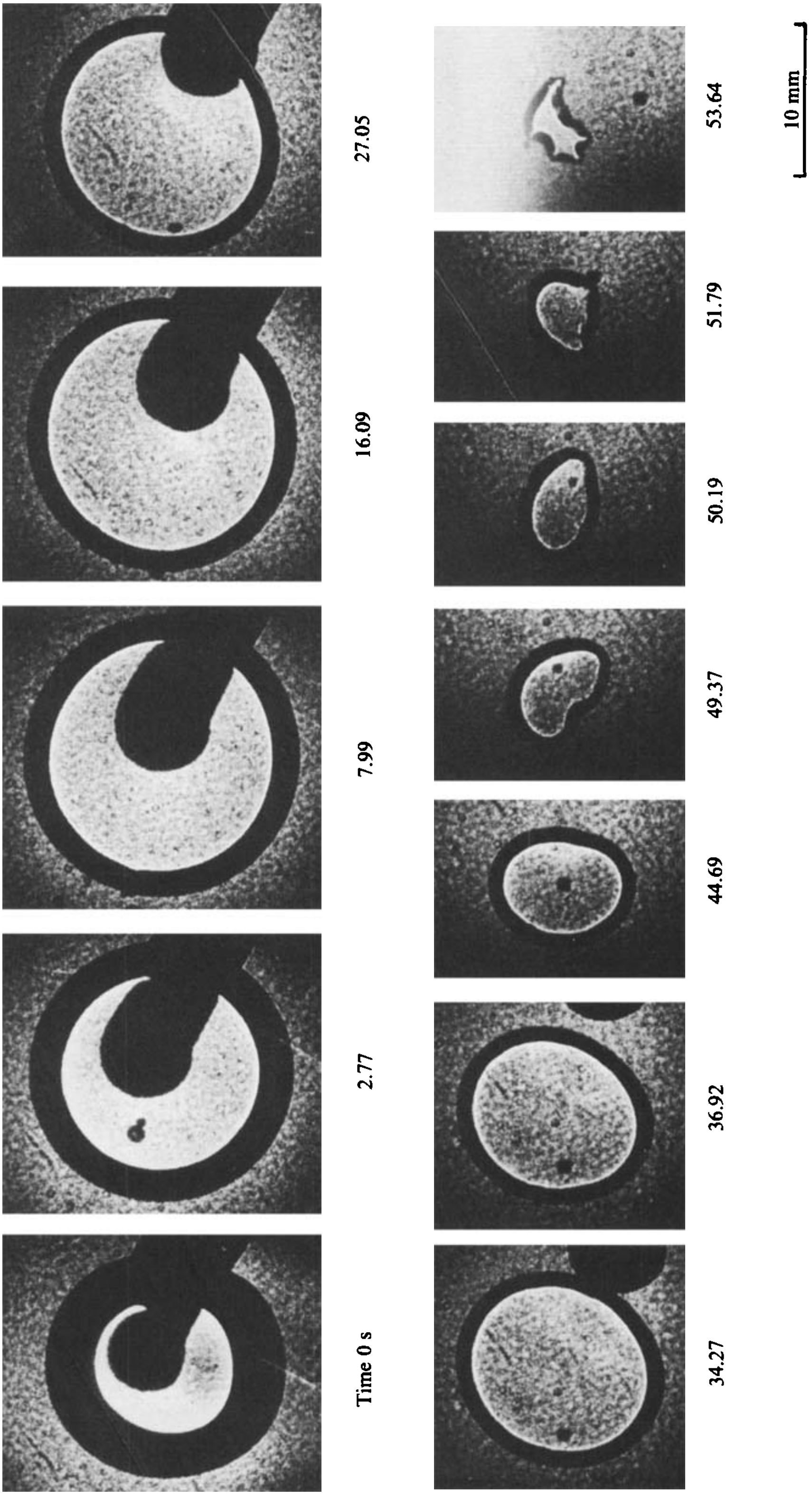

FIGURE 6. Shadowgraphs of an evaporating lens. Run F-11 (see figure 3).

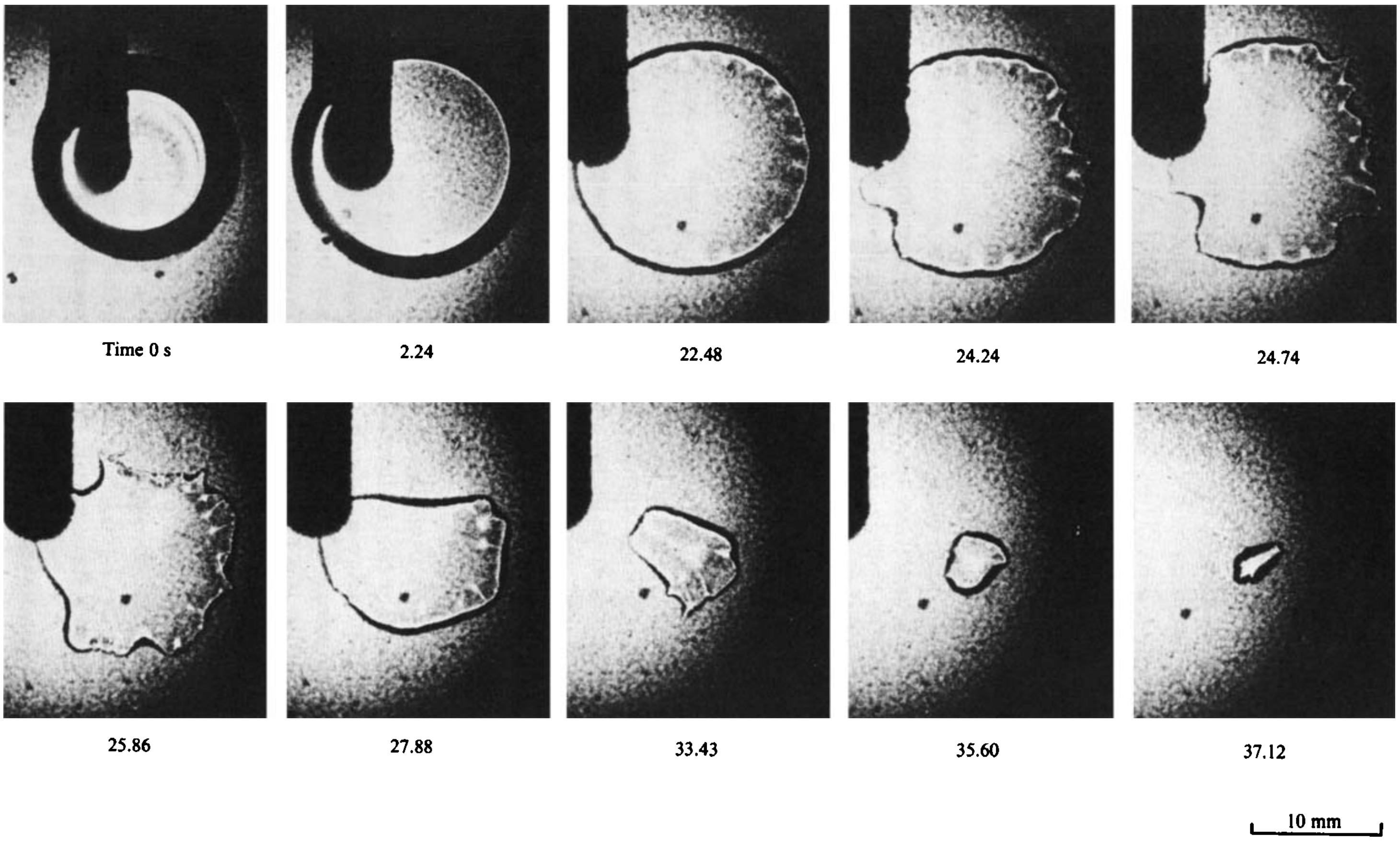

FIGURE 7. Shadowgraphs of an evaporating lens. Run F-16 (see figure 3).

for spreading reduces. After the adsorption is completed at the end of stage I, drops turn into lenses without exhibiting the initial spreading when they burst. Hypothesis (ii)[†] assumes that the adsorption is completed before the first drop is fed to the water surface and that *n*-pentane liquid intrinsically tends to spread,[‡] rather than to form a lens, on the water surface as long as it is free from contamination. A fixed quantity of contaminant is carried to the water surface by each *n*-pentane drop and is left to form a monolayer after the drop bursts and evaporates. Stage II begins at the point at which the *n*-pentane liquid no longer spreads against the contaminant monolayer and is thus confined to a lens. These hypotheses should be assessed by future examination.

3.2. *Dependence on fluid-sample purities*

The ageing effect described in the preceding subsection has also been studied with systems B and C listed in table 1. The results are shown in figure 8. In these experiments a large number, up to 200, of drops were sometimes supplied to the water surface between taking two successive data sets in order to hasten the ageing and thus to shorten the experimental time, which would be otherwise excessively long. Because of this, we have selected the total number of drops supplied to the surface instead of the time lapse as a measure of the ageing in figure 8. The changes in t_v with age in systems B and C are apparently different from that in system A shown in figure 3, though an exact comparison on the rate of ageing is impossible; and they are different from each other as well. In the case of system B, there is no stage corresponding to stage II. For system C, we can recognize only two stages, corresponding to stage I and stage IV respectively. Corresponding to these facts the behaviours of lenses in both of these cases are similar, except in the first stage corresponding to stage I, to those observed in stages III and IV in case of system A. All of the aforementioned findings indicate that the water surface in a system of lower purity ages more rapidly than that in a system of higher purity, supporting the view that such an ageing of the water surface, possibly except in the first stage in which the adsorption of *n*-pentane molecules may still be incomplete, should be ascribed to an accumulation of some contaminants at the water surface. Since a noticeable difference in the ageing characteristics is observed when replacing either the *n*-pentane sample or the water sample, we can conclude that such contaminants are released in part from each.

We could neither identify the contaminants in question nor show clearly the mechanism by which the contaminants affect the evaporation of lenses, but would like to suggest the following. When a *n*-pentane drop bursts at the water surface and turns into a lens, its top surface (*n*-pentane/vapour interface) and bottom surface (water/*n*-pentane interface) are both newly formed except probably for a small fraction of the latter. These surfaces must therefore be fairly clean immediately after the lens formation irrespective of the age of the water surface and the contaminant concentration in the bulk of each liquid phase. With the time lapse, contaminant molecules diffuse toward each surface from two phases separated by the surface and, crossing the three-phase contact line, from the external water surface. If these molecules adsorb at, for example, the bottom surface resulting in a decrease

---

[†] This hypothesis was originally presented by a referee as an alternative to hypothesis (i) which was originated by ourselves.

[‡] This assumption does not necessarily lead to the intriguing conclusion that the equilibrium spreading coefficient of *n*-pentane on water is positive. Note that the water surface of interest here is in contact with *n*-pentane vapour whose pressure is lower than the saturation pressure of *n*-pentane at the temperature T_∞ while $T_\infty > T_s$.

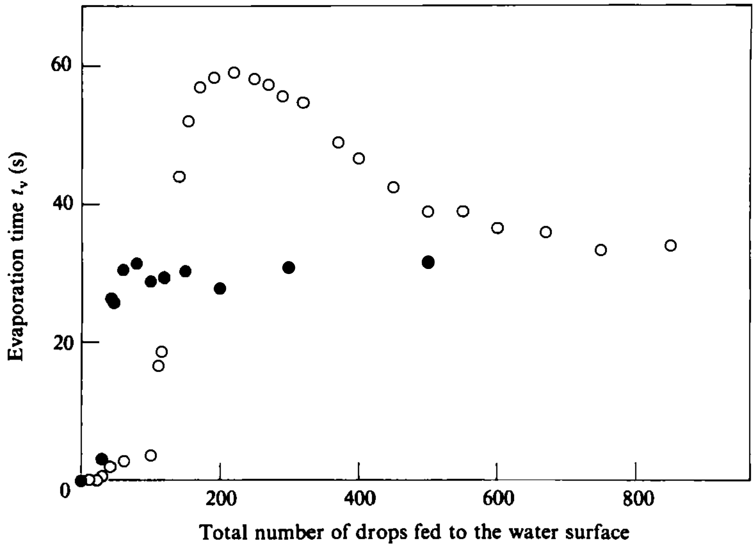

FIGURE 8. Variation of evaporation time with total number of drops fed to the water surface for systems B and C: $V_0 = 48$ mm^3; ○, system B, $\Delta T = 2.7 \sim 3.6$ K; ●, C, $\Delta T = 2.9 \sim 3.3$ K.

of the interfacial tension to some extent, the lens will tend to spread with an increasing diameter D. The diffusion/adsorption process is generally time consuming, and therefore D will increase gradually with time; this is consistent with the lens behaviour observed in stages III and IV in system A and also in any stages after the first one in system B or C. The erratic deformation of lenses as demonstrated in figures 6 and 7 should be ascribed to a non-uniform (and possibly time-dependent) distribution of the tension at each surface, which in turn results from a non-uniform adsorption of the contaminant molecules.

3.3. *Dependence on temperature difference*

Figure 9 shows the dependence of the evaporation time t_v on the temperature difference $\Delta T (= T_\infty - T_s)$. The data employed here are only those taken with system A in stage II. The data scatter is quite small compared with those given in previous reports (Bentwich, Landau & Sideman 1970; Kodres, Jacobs & Boehm 1979; Kaneko 1982). (Bentwich *et al.* showed their data not in the form of the t_v *vs* ΔT relation but as $\mathrm{d}R/\mathrm{d}t$ *vs* ΔT, where R is lens radius and t is time.) This is understandable considering that data taken in different stages were employed indiscriminately in one of the previous studies (Kaneko 1982) and were presumably the same in the other two. Among those previous studies, Kodres *et al.* (1979) showed data with a relatively narrow scatter compared with the rest. This may be because they used tap water instead of distilled water, and the ageing effect is presumably less significant with tap water.

Figure 10 summarizes some lens-diameter histories. These histories were obtained with system A, exclusively in stage II, but at different ΔT's. We can recognize on this figure that the initial lens diameter decreases with an increase of ΔT. In other words, the initial thickness δ_0 of a lens averaged over its projected area on a horizontal plane is larger at larger ΔT; this is demonstrated in figure 11.

The dependence of δ_0 on ΔT as shown in figure 11, as well as the change of the average lens thickness deviating from δ_0 in each evaporation process as stated before,

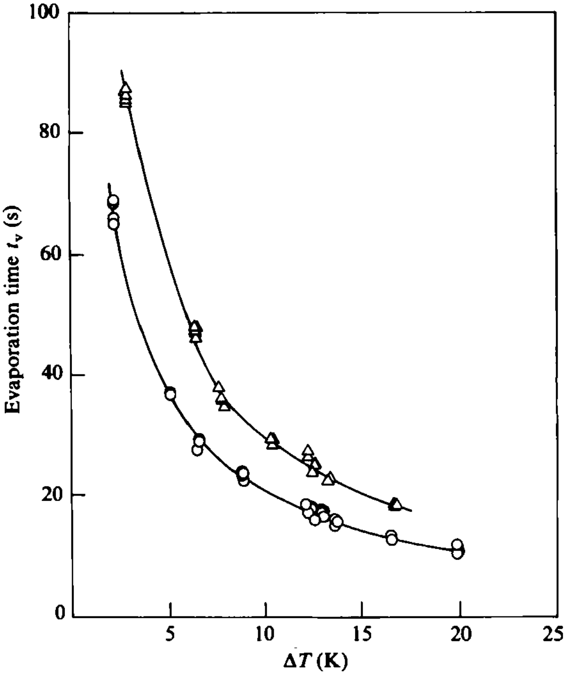

FIGURE 9. Dependence of evaporation time in stage II, system A, on the temperature difference: ○, $V_0 = 14 \sim 16$ mm³; △, $47 \sim 50$ mm³.

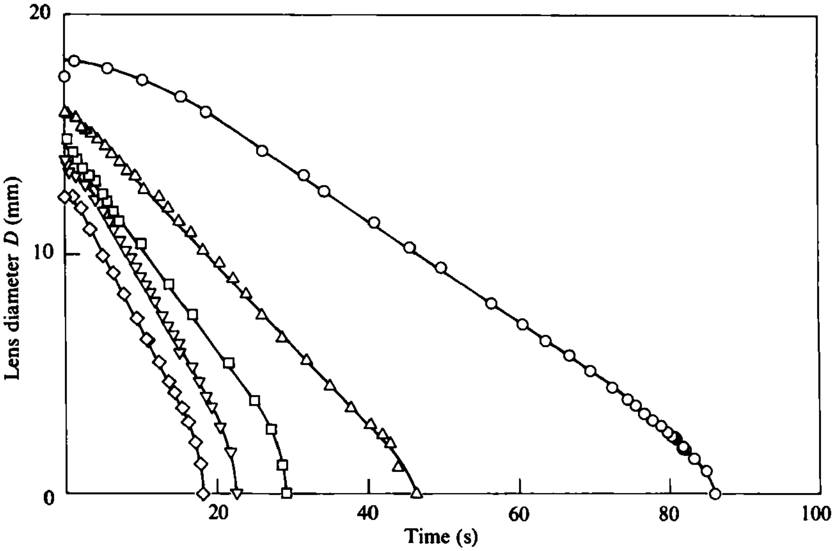

FIGURE 10. Variation with temperature difference of lens-diameter histories in stage II, A: $V_0 = 47 \sim 50$ mm³; ○, $\Delta T = 2.9$ K; △, 6.5; □, 10.5; ▽, 13.3; ◇, 16.7.

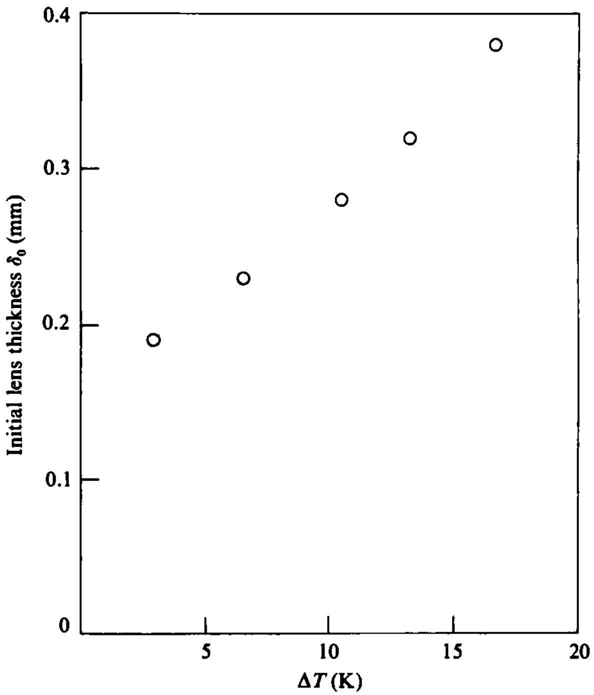

FIGURE 11. Dependence of initial, average lens thickness on the temperature difference; $V_0 = 47 \sim 50\ \mathrm{mm}^3$

poses a serious question about the validity of analyses of heat transfer to lenses made in previous studies. In every previous study it was assumed that the thickness of a lens did not change over its life and did not depend on ΔT; and accordingly a unique, constant thickness was employed, which was determined by evaluating experimentally the initial thickness of some lenses at a certain level of ΔT. Thus, some results in the previous studies deduced using the assumption of constant lens thickness may involve appreciable errors.

3.4. *Cellular convection inside lenses*

At ΔT's higher than 6 K, we could recognize on laser shadowgraphs a cellular convection inside lenses. Figure 12 shows a typical sequence taken early in stage II with system A. A cellular convection generally appeared within 1 s after the formation of each lens, and after some time lapse it faded away. The period in which the convection could be recognized in each lens life shortened appreciably with increasing age of the water surface even within stage II, and lengthened with an increase of ΔT. The increase of ΔT also resulted in larger cells with more irregular shapes. Some of the cells in each lens exhibited lively, erratic migrations particularly at higher ΔT.

It may be worthwhile to show the critical condition for the inception of the cellular convection in terms of Rayleigh number defined as $Ra = g\beta\delta_0^3\,\Delta T/(\kappa\nu)$, where g is the acceleration of gravity, β thermal-expansion coefficient, κ thermal diffusivity and ν kinematic viscosity. The physical properties β, κ and ν are of n-pentane and can be evaluated at T_s for the present purpose. The temperature difference ΔT is used as proxy for the unknown temperature difference $(T_i - T_s)$ over the lens thickness. The

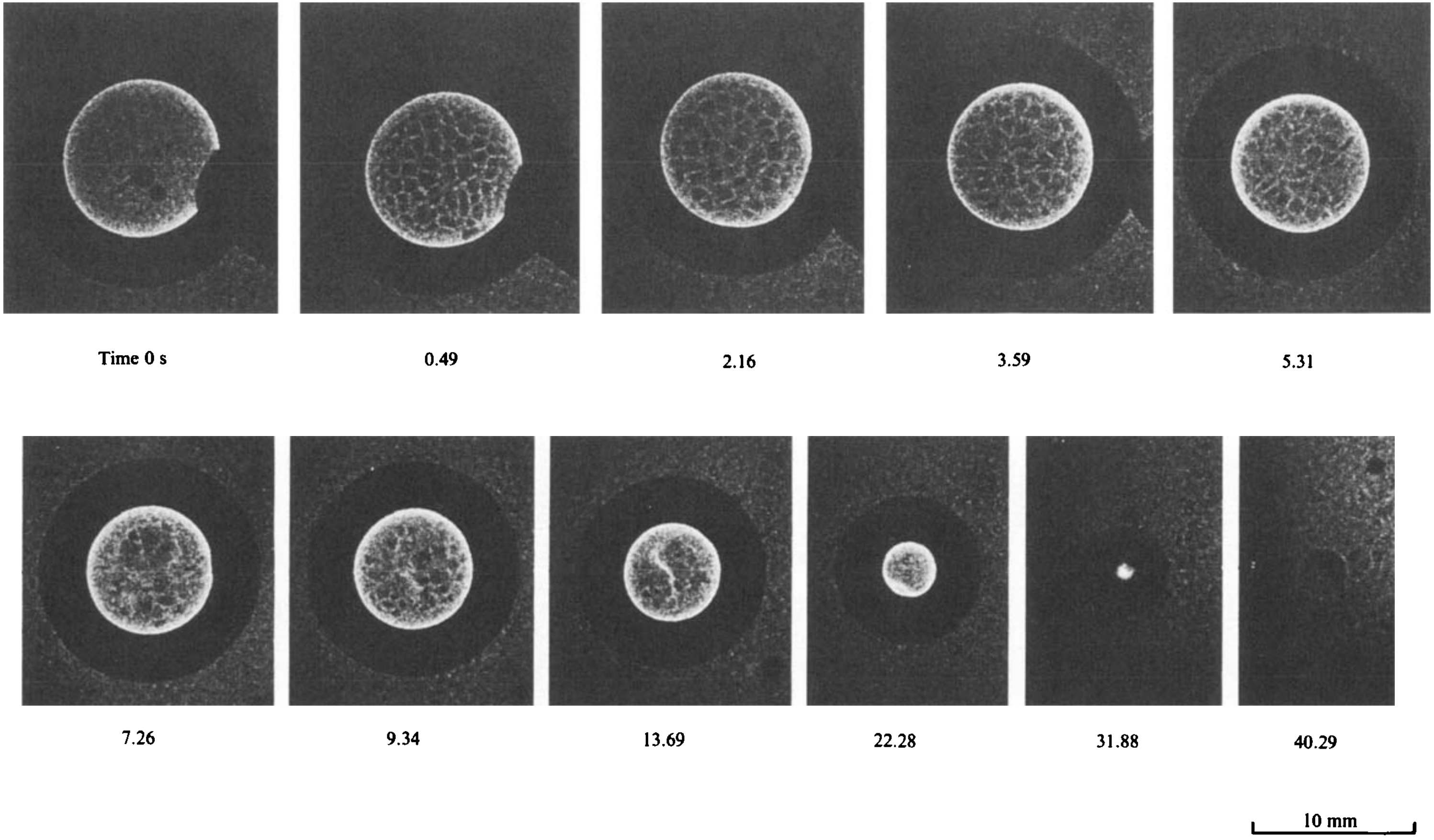

FIGURE 12. Shadowgraphs of an evaporating lens: $V_0 = 49$ mm^3; $\Delta T = 6.5$ K. Cellular convection can be recognized in the lens.

critical value of *Ra* is calculated to be about 50, which is lower than critical values predicted theoretically for a liquid layer, one or both of whose surfaces are free to move (Sparrow, Goldstein & Jonsson 1964; Chandrasekhar 1981). It would be much lower than 50 if we used $(T_1 - T_s)$ instead of ΔT. Such a low value of critical Rayleigh number could not be explained unless the onset of the cellular convection is due not only to buoyancy but also to a larger extent to Marangoni force. The Marangoni force working at either the top or bottom surface of a lens is possibly originated by a non-uniform temperature along the surface. The non-uniform temperature along the top surface must be accompanied by a non-uniform partial pressure along the surface of *n*-pentane vapour, which is complemented by a non-uniform partial pressure of water vapour. The maximum range of possible temperature variations at the top surface is established by the lower limit T_s and the upper limit T_{1s} as stated in §2. The corresponding temperature variation along the bottom surface must be much smaller than that at the top surface, because the bottom surface contacts with the water, not with the vapour mixture, which has a much higher thermal conductivity. For the abovementioned reason as well as the stronger temperature dependence of pentane/vapour interfacial tension than that of water/pentane interfacial tension (Mori, Tsui and Kiyomiya 1984), we can reasonably presume that the Marangoni force working at the top surface has a much larger magnitude than that at the bottom surface and thus serves as the major driving force for the cellular convection. If this is the case, the Marangoni force at the bottom surface does not promote but, rather, counteracts the convection.

The cellular convection inside a lens as discussed above must cause a reduction in the resistance to heat flow crossing the lens to its top surface. It should also be noted that such a convection inside a lens may possibly be accompanied by a conjugate convection in the substrate water phase underneath the lens, which would cause a reduction of the resistance in the substrate phase. These convection effects need future evaluation.

4. Concluding remarks

This experimental study has revealed that lens evaporation is a phenomenon bearing more complex and more critical relations with surface and interfacial conditions than has been assumed in previous studies. The most remarkable finding in this study may be that the behaviour of lenses as well as their evaporation rate changes with the age of the substrate-liquid surface in a particular way. If experimental data were taken at various surface ages with no distinction in previous studies, their wide scatter as discussed in §1 would be no more than a natural consequence. The failure of the prediction of evaporation rate by the previous theoretical models may well be ascribed to the thinning of lenses during their evaporation and their irregular oscillatory motion, both of which become more conspicuous with an increase in the surface age.

The ageing effect also has an important implication for the designing of practical direct-contact evaporators, for which there are many possible configurations. Depending on the configuration, the substrate-liquid surface can be renewed with various frequencies or may never be renewed throughout the period of each continuous operation. A difference in the surface-renewal frequency presumably yields an appreciable difference in the evaporator performance, a point which should be taken into account in optimum evaporator design.

This work has been subsidized in part by a Grant in Aid for Scientific Research from the Ministry of Education, Science and Culture of Japan (Grant 59550160). We are indebted to S. Endoh and N. Kurose, students at the Department of Mechanical Engineering, Keio University, for their assistance in a part of the experimental work. We appreciate helpful comments from the referees, some of which were reflected in this paper. Particularly detailed comments concerning surface contamination given by one of the referees were very instructive and provided us with an opportunity to reconsider more carefully some problems from the aspect of surface chemistry.

REFERENCES

BENTWICH, M., LANDAU, U. & SIDEMAN, S. 1970 Direct contact heat transfer with change of phase: evaporation of discrete volatile films from the surface of a stagnant immiscible liquid. *Intl J. Heat Mass Transfer* **13**, 945–956.

CHANDRASEKHAR, S. 1981 *Hydrodynamic and Hydromagnetic Stability*, pp. 34–36. Dover.

DETWILER, A. & BLANCHARD, D. C. 1978 Aging and bursting bubbles in trace-contaminated water. *Chem. Engng Sci.* **33**, 9–13.

HIGETA, K., MORI, Y. H. & KOMOTORI, K. 1979 Condensation of a single vapor bubble rising in another immiscible liquid. *AIChE Symp. Ser.* **75**–189, 256–265.

IAPS (International Association of the Properties of Steam) 1976 Release on *Surface Tension of Water Substance.*

KANEKO, M. 1982 Heat transfer to an evaporating lens of volatile liquid floating on a stagnant immiscible liquid (in Japanese). M.Engng thesis, Keio University, Yokohama.

KANEKO, M. & MORI, Y. H. 1984 Evaporation of a volatile-liquid lens floating on the surface of a stagnant immiscible liquid. *Intl Comm. Heat Mass Transfer* **11**, 209–218.

KITCHENER, J. A. & COOPER, C. F. 1959 Current concepts in the theory of foaming. *Q. Rev.* **13**, 71–97.

KODRES, C. A., JACOBS, H. R. & BOEHM, R. F. 1979 Heat transfer to an evaporating, floating lens. *ASME Paper* 79-HT-13. Presented at the 18th Nat. Heat Transfer Conf., San Diego, Calif.

KODRES, C. A., JACOBS, H. R. & BOEHM, R. F. 1980 A numerical method for determining direct-contact heat transfer rates to a superheated evaporating floating droplet. *Numer. Heat Transfer* **3**, 21–34.

LANGMUIR, I. 1933 Oil lenses on water and the nature of monomolecular expanded films. *J. Chem. Phys.* **1**, 756–776.

MORI, Y. H., TSUI, N. & KIYOMIYA, M. 1984 Surface and interfacial tensions and their combined properties in seven binary, immiscible liquid–liquid–vapor systems. *J. Chem. Engng Data* **29**, 407–412.

MYSELS, K. J. & FLORENCE, A. T. 1970 Techniques and criteria in the purification of aqueous surfaces. In *Clean Surfaces: Their Preparation and Characterization For Interfacial Studies* (ed. G. Goldfinger), pp. 227–268. Marcel Dekker.

SPARROW, E. M., GOLDSTEIN, R. J. & JONSSON, V. K. 1964 Thermal instability in a horizontal fluid layer: effect of boundary conditions and non-linear temperature profile. *J. Fluid Mech.* **18**, 513–528.

YANG, W.-J. & NOURI, A. 1981 Interfacial turbulence in minute drops evaporating on a flat plate. *Lett. Heat Mass Transfer* **8**, 115–125.